Dissection and manipulation of antigen-specific T cell responses

Schepers, K.

Chapter 2

Differential kinetics of antigen-specific $CD4^+$ and $CD8^+$ T cell responses in the regression of retrovirus-induced sarcomas

Koen Schepers, Mireille Toebes, Gitte Sotthewes, Florry A. Vyth-Dreese, Trees A.M Dellemijn, Cornelis J.M. Melief, Ferry Ossendorp, and Ton N.M. Schumacher

J. Immunol. 169:3191-3199 (2002)

Differential Kinetics of Antigen-Specific CD4$^+$ and CD8$^+$ T Cell Responses in the Regression of Retrovirus-Induced Sarcomas[1]

Koen Schepers,* Mireille Toebes,* Gitte Sotthewes,* Florry A. Vyth-Dreese,* Trees A. M. Dellemijn,* Cornelis J. M. Melief,† Ferry Ossendorp,† and Ton N. M. Schumacher[2]*

Despite the accepted role for CD4$^+$ T cells in immune control, little is known about the development of Ag-specific CD4$^+$ T cell immunity upon primary infection. Here we use MHC class II tetramer technology to directly visualize the Ag-specific CD4$^+$ T cell response upon infection of mice with Moloney murine sarcoma and leukemia virus complex (MoMSV). Significant numbers of Ag-specific CD4$^+$ T cells are detected both in lymphoid organs and in retrovirus-induced lesions early during infection, and they express the 1B11-reactive activation-induced isoform of CD43 that was recently shown to define effector CD8$^+$ T cell populations. Comparison of the kinetics of the MoMSV-specific CD4$^+$ and CD8$^+$ T cell responses reveals a pronounced shift toward CD8$^+$ T cell immunity at the site of MoMSV infection during progression of the immune response. Consistent with an important early role of Ag-specific CD4$^+$ T cell immunity during MoMSV infection, CD4$^+$ T cells contribute to the generation of virus-specific CD8$^+$ T cell immunity within the lymphoid organs and are required to promote an inflammatory environment within the virus-infected tissue. ***The Journal of Immunology,*** **2002, 169: 3191–3199.**

The development of protective T cell immunity against intracellular pathogens involves MHC class I-restricted cytotoxic CD8$^+$ T cells and MHC class II-restricted helper CD4$^+$ T cells. Whereas the activity of Ag-specific CD8$^+$ T cell immunity primarily involves direct inactivation of Ag-expressing cells, the actions of Ag-specific CD4$^+$ T cell populations are more diverse. Traditionally, CD4$^+$ T cells are considered to provide a setting for optimal CD8$^+$ T cell and B cell activation. Although originally this T cell help was thought to be mediated by Th-secreted cytokines, more recent studies have indicated that CD4$^+$ T cell help is at least in part mediated through the "licensing" of APCs for CD8$^+$ T cell activation (1–3). In addition to this role of CD4$^+$ T cell immunity in the initiation of cytotoxic T cell responses, CD4$^+$ T cells can also mediate other orchestrating functions, as well as direct effector functions in the control of (retro) viral infections (4) and tumors (5, 6). Despite these accepted roles for Ag-specific CD4$^+$ T cells in disease control, comparatively little is known about the development of CD4$^+$ T cell immunity.

In the past few years, MHC class I multimers have been extensively used to study CD8$^+$ T cell responses in a number of tumor and virus models (7, 8). These studies have provided insight into fundamental characteristics of CD8$^+$ T cell immunity, such as the magnitude, distribution, and kinetics of CD8$^+$ T cell responses during pathogen encounter. More recently, MHC class II multimers have been used to study the presence of Ag-specific CD4$^+$ T cells in different models. These studies showed the presence of small but demonstrable numbers of Ag-specific CD4$^+$ T cells in mice vaccinated with model Ags and in the synovial fluid of individuals suffering from chronic Lyme arthritis and rheumatoid arthritis (9–12). In addition, virus-specific CD4$^+$ T cells have been detected in the blood of patients exposed to HSV or influenza A virus, after specific in vitro expansion of PBMCs (13, 14). Recently, Homann et al. (15) used MHC class II and class I tetramers to address the formation and stability of CD4$^+$ and CD8$^+$ T cell memory upon infection of mice with lymphocytic choriomeningitis virus (LCMV)[3] and demonstrated that, whereas CD8$^+$ T cell memory is stably maintained for life, CD4$^+$ T cell memory declines gradually.

Here, we use an onco-retrovirus infection model to study the development of primary Ag-specific T cell immunity. Upon infection of mice with Moloney murine sarcoma and leukemia virus complex (MoMSV), animals rapidly develop pronounced virally-induced sarcomas. These lesions are characterized by a mixture of virus-infected myocytes and a large infiltrate of lymphocytes, granulocytes, and macrophages (16–18). In immunocompetent mice, the virus-induced lesions regress in a T cell-dependent manner over a period of 4–5 wk. In contrast, immunodeficient mice succumb as a consequence of uncontrolled viral spreading/cellular transformation by the mos oncogene that is encoded by this onco-retrovirus (19–21). Importantly, CD4$^+$ T cell immunity is essential for successful viral clearance upon MoMSV infection, as shown by the fact that CD4-depleted mice develop progressive and

*Department of Immunology, The Netherlands Cancer Institute, Amsterdam, The Netherlands; and †Department of Immunohematology and Blood Transfusion, Leiden University Medical Center, Leiden, The Netherlands

Received for publication March 28, 2002. Accepted for publication July 9, 2002.

The costs of publication of this article were defrayed in part by the payment of page charges. This article must therefore be hereby marked *advertisement* in accordance with 18 U.S.C. Section 1734 solely to indicate this fact.

[1] This work was supported by the Dutch Cancer Society (Grants NKI 99-2036 and NKI 2000-2248) and the Netherlands Organization for Scientific Research (Grant NWO 901-07-226).

[2] Address correspondence and reprint requests to Dr. Ton N. M. Schumacher, Department of Immunology, The Netherlands Cancer Institute, Plesmanlaan 121, 1066 CX, Amsterdam, The Netherlands. E-mail address: tschum@nki.nl

[3] Abbreviations used in this paper: LCMV, lymphocytic choriomeningitis virus; MoMSV, Moloney murine sarcoma and leukemia virus complex; H19-Env, I-A^b-restricted MoMSV-envelope epitope; NP, nucleoprotein; GagL*, the GagL$_{85–93}$ peptide variant Abu-Abu-Leu-Abu-Leu-Thr-Val-Phe-Leu; D^b-GagL* tetramer, H-2D^b tetramer containing the GagL* peptide; FMR, Friend/Moloney/Rauscher; I-A^b-Env tetramer, I-A^b tetramer containing the H19-Env peptide; DLN, draining lymph node; HAU, hemagglutinating unit; IHC, immunohistochemistry.

lethal lesions (Refs. 22 and 23 and see *Results*). Furthermore, vaccination with a Moloney-derived T helper epitope protects mice from retrovirus-induced tumors (24). Consequently, analysis of the MoMSV-specific $CD4^+$ T cell response may provide insights into the characteristics of a successful retrovirus-specific immune response and the development and function of Ag-specific $CD4^+$ T cell immunity in general.

Materials and Methods

Mice, viruses, and Abs

C57BL/6 mice were bred at the experimental animal department of the Netherlands Cancer Institute (Amsterdam, The Netherlands) and at the Leiden University Medical Center animal facility (Leiden, The Netherlands). Mice were kept under specified pathogen-free conditions. Mice were handled at all times in accordance with institutional guidelines.

MoMSV was prepared and injected (10^3 focus-forming units) in the thigh muscle as described (25). Purified recombinant influenza A virus strain A/NT/60/68 was kindly provided by Dr. R. Consalves (National Institute of Medical Research, London, U.K.). A/NT/60/68 virus was grown and hemagglutination activity and infectious titers were tested in the Department of Virology, Erasmus University (Rotterdam, The Netherlands). The mAbs used for in vivo depletion of the $CD4^+$ and $CD8^+$ T cell subsets were GK1.5 and 2.43, respectively. Purified Abs were administered by i.p. injection of 100 μg of Ab in 0.2 ml of PBS at the time points indicated in the figures. These treatments efficiently deplete the respective T cell subsets (depletion efficiency: $CD4^+$ cells, 99%; $CD8^+$ cells, 95%; data not shown). $CD4^+CD8^+$ cell levels stay strongly decreased for >2 wk after withdrawal of Ab treatment. Abs used for flow cytometry were PE- and allophycocyanin-conjugated anti-CD4 Ab, FITC-conjugated anti-CD62L, anti-CD44 and anti-CD43 (1B11) Ab (BD Biosciences, Mountain View, CA), R-PE/Cy5-conjugated F4/80 Ab (Serotec, Oxford, U.K.), and allophycocyanin-conjugated anti-CD8a Ab (BD Biosciences). Abs used for in situ analysis were biotin-conjugated anti-CD4 (L3T4), anti-CD8b.2, and anti-I-A^b, and FITC-conjugated anti-CD11c (BD Biosciences) and F4/80 Ab (Serotec).

Generation of tetramers

Peptides were produced using standard F-moc chemistry. PE-labeled H-$2D^b$ tetramers were produced as described previously (26, 27) and stored frozen in TBS/16% glycerol/0.5% BSA.

Allophycocyanin-labeled I-A^b tetramers were generated using MHC class II heterodimers expressed either in COS-7 cells or in insect cells. An α-chain construct comprising the signal peptide and the extracellular domain of the α-chain, followed by a six-residue GGS-linker, an acid leucine zipper, and a his tag, was assembled from the following oligos: 5′-GGTGTC GACGCCACCATGCCGTGCAGCAGAGC-3′ (contains *Sal*I site), 5′-TTTTTCCAGCGCCTGCAGTTCTTTTTCCAGCTGCGCGGAACCACC GGAACCACCCTCAGGTTCCCAGTGTTTCAG-3′, 5′-CTGCAGGCGC TGGAAAAAGAAAACGCGCAGCTGGAATGGGAACTGCAGGCG-3′, and 5′-CCGAATTCTTAGTGGTGGTGGTGGTGGTGACCACCCTGCG CCAGTTCTTTTTCCAGCGCCTGCAGTTCCCATTC-3′ (contains *Eco*RI site). A β-chain construct comprising the signal peptide of the β-chain, a *Bam*HI cloning site, a nine-residue GGS-linker, and amino acid GD SERH. . . EWRAQS of the extracellular domain of the β-chain, followed by a six-residue GGS-linker, basic leucine zipper, and a biotag was assembled from the following oligos: 5′-GGTGTCGACGCCACCATGGC TCTGCAGATCCCC-3′ (contains *Sal*I site), 5′-CAGAGCCTGGAGTTT CTTCTTCAGCTGGGCGCTACCACCGGAGCCGCCAGACTGTGCCC TCCACTC-3′, 5′-GAAGAAGAAACTCCAGGCTCTGAAAAA, 5′-AAA GAATGCCCAGCTCAAGCAGAAGCTGCAGGCCCTGAAGAAA-3′, 5′-CGAAGATGTCGTTCAAACCACCACCCGCGGAACCACCGGAACCCT GAGCCAGCTTTTTCTTCAGGGCCTGCAG-3′, 5′-GGTTTGAACGACA TCTTCGAAGCTCAGAAAATCGAATGG-3′, 5′-ACCGAATTCTTAGTG CCATTCGATTTTCTGAGC-3′ (contains *Eco*RI site), 5′-GTCTCCGGAG CCGCCGCTACCACCGGATCCGCCCTCAGTCCT/CTGGGC-3′, and 5′-GGCGGCTCCGGAGACTCCGAAAGGCATTTC-3′. The *Bam*HI site was used to insert an I-A^b-restricted MoMSV-envelope epitope (H19-Env) peptide-encoding (EPLTSLTPRCNTAWNRLKL) sequence (using primers 5′-GATCCGAGCCACTGACCAGCCTGACCCCAAGATGCAACACCGCTT GGAACAGACTGAAGCTGG-3′ and 5′-GATCCCAGCTTCAGTCTGTT CCAAGCGGTGTTGCATCTTGGGGTCAGGCTGGTCAGTGGCTCG-3′) or a nucleoprotein $(NP)_{413–435}$ peptide-encoding sequence (using primers 5′-GATCCGTTCAGCGTAACCTGCCGTTCGACAAACCGACCATCATGG CTGCTTTCACCGGTAACACCTACG-3′ and 5′-GATCCGTAGGTGTTA CCGGTGAAAGCAGCCATGATGGTCGGTTTGTCGAACGGCAGGTTA CGCTGAACG-3′). The α- and β-chain were cloned into the eukaryotic expression vectors pMT2 and pMT/V5-HisA (Invitrogen, San Diego, CA). The resulting pMT2 plasmids were transiently transfected (5 μg of each plasmid) into COS-7 cells by standard DEAE transfection. After DMSO shock, cells were cultured for 72 h at 37°C in 1× Hybridoma medium NS (Boehringer Mannheim, Mannheim, Germany) in IMDM (Life Technologies, Paisley, U.K.). For production in insect cells, the resulting pMT/V5-HisA plasmids (9.5 μg of each plasmid) were transfected into *Drosophila* S2 cells together with pS2Neo (1 μg). Stable transfectants were selected by growing the cells in SDM medium (Life Technologies) containing 10% FCS and 2 mg/ml G418 for 3–4 wk. The $\alpha\beta$ heterodimer production was induced by growing the cells in the presence of 500 μM Cu_2So_4 for 4–5 days. Subsequently, the supernatant was collected and concentrated, and the buffer was exchanged to 100 mM NaCl, 20 mM Tris (pH 8). The $\alpha\beta$ heterodimers were purified by Co^{2+} precipitation using 100 mM Imidazole for elution. Then $\alpha\beta$ heterodimers were biotinylated with BirA, purified, and converted to tetramers as has been described for MHC class I tetramers (27). MHC class II tetramers were stored at 4°C in 150 mM NaCl/20 mM Tris (pH 7)/0.5% BSA (Sigma-Aldrich, The Netherlands). MHC class II tetramers were used at a final concentration of ~0.75 μg/ml.

Cell isolation and in vitro restimulation

Spleen, lymph nodes, and lungs were isolated and homogenized using a nylon mesh filter (NPBI, Emmer-Compascuum, The Netherlands). Tumors were isolated and homogenized by treatment of small tumor pieces with Collagenase (1 mg/ml) and DNase (10 μg/ml) for 30 min at 37°C and were transferred through a nylon mesh filter. RBCs were removed from the cell suspensions by treatment with erylysis buffer (155 mM NH_4Cl, 10 mM $KHCO_3$, and 0.1 mM EDTA (pH 7.4)).

For in vitro restimulation, cells were labeled with CFSE (Molecular Probes, Leiden, The Netherlands) as described (28). CFSE-labeled cells were stimulated for 6 days in IMDM supplemented with 10% FCS (Bio-Whittaker, Verviers, Belgium), 0.5 μM 2-ME (Merck, Hohenbrunn, Germany), penicillin (100 U/ml), and streptomycin (100 μg/ml) (Boehringer Mannheim) (culture medium) in either the presence or absence of H19-Env peptide.

Flow cytometry

MHC class I tetramer staining was performed in PBS containing 0.5% BSA and 0.02% NaN_3 at room temperature for 15 min. MHC class II tetramer staining was performed in culture medium at 37°C for 3–3.5 h. Staining with Abs was performed during the last 20 min of tetramer staining. Samples were also stained with F4/80 Ab to be able to reduce background staining of MHC class II tetramers by gating out macrophages. Subsequently, cells were washed and resuspended in PBS containing 0.2% BSA and 0.02% NaN_3. Before analysis, propidium iodide was added to select for propidium iodide-negative (living) lymphocytes. Analysis was performed on a FACSCalibur using CellQuest software (BD Biosciences).

Intracellular staining

Intracellular staining was performed as described (29). In brief, cells were incubated with peptide (10 μg/ml) for 4–5 h at 37°C in the presence of recombinant human IL-2 (10 U/ml) and brefeldin A (1 μl/ml). After incubation, cells were stained with anti-CD8a-allophycocyanin or anti-CD4-allophycocyanin Ab, incubated in Cytofix/Cytoperm solution (BD Biosciences) for 20 min on ice, washed, and stained for intracellular cytokine with anti-IFN-γ-FITC (BD Biosciences) or FITC-labeled isotype-matched control Ab (BD Biosciences). Analysis was performed on a FACSCalibur using CellQuest software (BD Biosciences).

Statistical analysis

Percentages and absolute numbers of tetramer-positive cells were logarithmically transformed, and subsequently a repeated measurement ANOVA was used. The model was fitted using restricted maximum likelihood, assuming constant SDs over cell type as well as time. SEs and p values were calculated using the sandwich estimator for the covariance matrix of the means. The p values were calculated from approximate type III F-tests, confidence intervals from approximate t-distributions. First, an overall test was done to determine whether the two curves differ in shape (cell*time interaction). If this was the case ($p < 0.05$), relative changes between adjacent days were estimated and compared between the two cell types. PROC MIXED of the SAS statistical was used for the analyses.

For statistical analysis of CD4-depleted and control mice, percentages of H-$2D^b$ tetramer containing the $GagL_{85–93}$ peptide variant Abu-Abu-Leu-Abu-Leu-Thr-Val-Phe-Leu (GagL*) peptide (D^b-GagL* tetramer)-positive cells were logarithmically transformed and analyzed by a Student's t test.

In situ immunohistochemical and immunofluorescence analysis

Cryostat fragments of retrovirus-induced sarcoma tissues were cut in 4-μm sections, air-dried overnight, and fixed in acetone for 10 min at room temperature. Sections were preincubated in 5% (v/v) normal goat serum (Central Laboratory of the Netherlands Red Cross Blood Transfusion Service, Amsterdam, The Netherlands), or 5% (v/v) normal mouse serum in case of staining with hamster Abs.

For immunohistochemical analysis, sections were stained using a standard alkaline phosphatase protocol as described previously, with slight modifications (30). Briefly, sections were stained with primary Ab diluted in PBS containing 1% BSA (plus 10% normal mouse serum in case of staining with hamster Abs). Sections stained with FITC-conjugated Ab were subsequently incubated with alkaline phosphatase-labeled sheep anti-FITC Ab (Boehringer Mannheim). Sections stained with biotin-conjugated Ab were subsequently incubated with streptavidin/biotin-conjugated alkaline phosphatase complex (ABC-protocol; DAKO, Glostrup, Denmark). Color was developed using naphtol AS-MX phosphate (0.3 mg/ml) plus New Fuchsin (0.1 mg/ml) in 0.2 M Tris-HCl buffer (pH 8.0; ABC-protocol; DAKO), and sections were counterstained with hematoxylin. Between incubation steps, sections were extensively rinsed in PBS. Within each staining procedure, isotype-matched control Abs were included and found negative.

Immunofluorescence double labeling was performed as described previously (31), with slight modifications. Briefly, sections were incubated with optimal dilutions of FITC-conjugated F4/80 Ab and biotin-conjugated mouse anti-mouse I-A^b (MHC class II) mAbs (in PBS containing 1% (w/v) BSA) for 1 h at room temperature, followed by incubation with Cy5-conjugated streptavidin (Jackson ImmunoResearch Laboratories, Palo Alto, CA). Confocal fluorescence images were obtained on a Leica TCS SP confocal system (Leica Microsystems, Heidelberg, Germany), equipped with an Ar/HeNe laser combination. Images were taken using a 40 $\times$ 1.25 NA objective. Color photomicrographs were taken from electronic overlays.

Results

Role of $CD4^+$ and $CD8^+$ T cells in the regression of MoMSV-induced sarcomas

After i.m. injection of mice with MoMSV virus, lesions develop within 2 wk, and they subsequently regress spontaneously. We determined the role of $CD4^+$ and $CD8^+$ T cells in immune control of MoMSV infection by analyzing lesion development in mice depleted for either $CD4^+$ cells or $CD8^+$ T cells. Consistent with earlier data (22, 23), CD4 depletion resulted in progressive outgrowth of MoMSV-induced lesions and subsequent death (Fig. 1), demonstrating that $CD4^+$ T cells are required for the regression of MoMSV-induced sarcomas. Mice depleted of $CD8^+$ cells show a delay in the regression of MoMSV-induced tumors but eventually clear the virus (Fig. 1) (22). Likewise, sarcoma regression is delayed but not abolished in perforin-deficient mice (32). Previously, it has been demonstrated that regression of MoMSV-induced lesions in immunodeficient mice can be achieved by infusion of Ag-specific $CD8^+$ T cell clones (33). Collectively, these data indicate that, whereas $CD4^+$ T cell immunity is crucial for the control of MoMSV infection, $CD8^+$ T cell immunity contributes to viral clearance in conjunction with CD8-independent mechanisms.

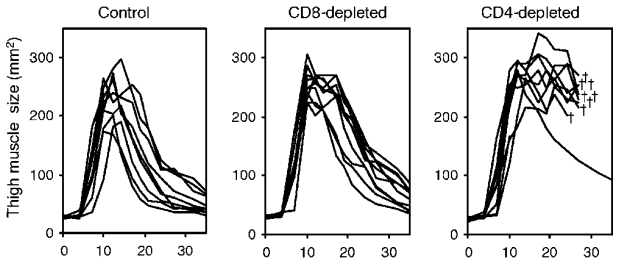

FIGURE 1. $CD4^+$ T cell-dependent regression of MoMSV-induced tumors. Mice were either left untreated (*left panel*) or injected i.p. with 100 μg of anti-CD8 Ab (2.43) (*middle panel*) or anti-CD4 Ab (GK1.5) (*right panel*) in 0.2 ml of PBS on days 0, 3, and 7. On day 0, mice were infected with MoMSV. Mice were monitored for thigh muscle size using a caliper measuring two perpendicular diameters. Each line represents one individual mouse. Animals were sacrificed when severely ill.

Detection of MoMSV-specific $CD4^+$ T cell immunity using MHC class II tetramers

Previously, Iwashiro et al. (34) defined the immunodominant I-A^b restricted epitope (H19-Env, EPLTSLTPRCNTAWNRLKL) of the envelope (gp70) protein of the Friend murine leukemia virus. This epitope is conserved in the Friend/Moloney/Rauscher (FMR) family of retroviruses that includes MoMSV. With the aim to visualize the Ag-specific $CD4^+$ T cell response during MoMSV infection, we generated I-A^b-tetramers containing the H19-Env epitope of MoMSV (I-A^b-Env). To this purpose, heterodimers of the extracellular domains of the I-A^b α-chain and β-chain were produced in eukaryotic cells with the H19-Env epitope covalently attached to the I-A^b β-chain. Velcro leucine zippers were included to promote heterodimerization (35), and a His-tag and biotinylation signal (bio-tag) were attached to the I-A^b α- and β-chain for subsequent purification and tetramer formation.

The specificity of the I-A^b-Env tetramers was first tested on H19-Env peptide-stimulated CFSE-labeled spleen cells of B6 mice that had previously been infected (40 days) with MoMSV. I-A^b-Env tetramers stained a sizeable percentage of $CD4^+$ spleen cells that had proliferated (i.e., were $CFSE^{low}$) on day 6 after stimulation with H19-Env peptide (Fig. 2*A*). Staining was found to be specific, as these $CD4^+CFSE^{low}$ cells did not stain with control I-A^b tetramers that contained an influenza A/NT/60/68 virus-derived peptide ($NP_{413-435}$, SVQRNLPFDKPTIMAAFTGNT) (36). Furthermore, after restimulation in the absence of the MoMSV Env-derived $CD4^+$ T cell epitope, little to no I-A^b-Env $tetramer^+$ T cells were detected within the $CD4^+CFSE^{low}$ population.

We subsequently tested the ability of the I-A^b-Env tetramer to detect Ag-specific T cells directly ex vivo. To this purpose, organs of MoMSV-infected mice were isolated on day 14 postinfection, and cell suspensions were stained with I-A^b-Env tetramers, anti-CD4, and phenotypic markers (Fig. 2*B*, shown for the 1B11 activation marker; see below). Low but detectable frequencies of I-A^b-Env $tetramer^+$ $CD4^+$ T cells are observed in the DLNs, spleen, and lesions of MoMSV-infected mice (average: 0.29, 0.50, and 1.09%, respectively) (Fig. 2*B*). Much lower levels of staining are observed in organs of both noninfected mice (average, 0.02 $\pm$ 0.01) and mice infected with the influenza A/NT/60/68 virus (average, 0.03 $\pm$ 0.01%) (Fig. 2*B*). Vice versa, $CD4^+$ T cells of MoMSV-infected mice did not stain with control I-A^b tetramers containing the influenza A NP-derived peptide (data not shown).

Detection of MoMSV-specific $CD8^+$ T cell immunity using MHC class I tetramers containing an altered peptide

Previously, Chen et al. (37) described the immunodominant $CD8^+$ T cell epitope of the FMR family of retroviruses (the H-2D^b-restricted MoMSV $GagL_{85-93}$ epitope, CCLCLTVFL). This H-2D^b-restricted epitope contains three cysteine residues that preclude the formation of MHC tetramers by their strong propensity to form disulfide-bonded dimers. To circumvent the problems associated with the inherent reactivity of this cysteine-rich epitope, we generated a set of variant peptides in which individual amino acids were replaced by the isosteric amino acid α-aminobutyric acid. Screening of variant peptides for their ability to induce IFN-γ secretion in $CD8^+$ T cells of MoMSV-infected mice by intracellular IFN-γ staining reveals that an H-2D^b-restricted MoMSV $GagL_{85-93}$ epitope variant in which all three cysteine residues were substituted by α-aminobutyric acid is recognized efficiently (data

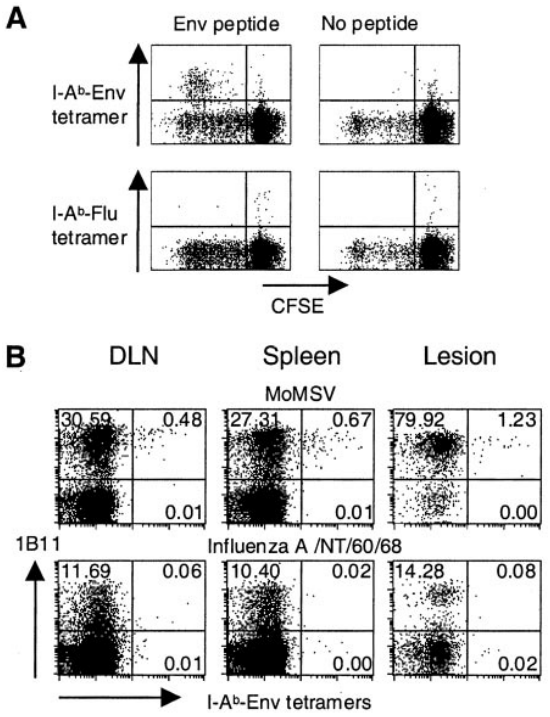

FIGURE 2. Detection of MoMSV-specific $CD4^+$ T cells. *A*, Purified spleen cells of mice previously infected (40 days) with MoMSV were labeled with CFSE and stimulated with or without H19-Env peptide. On day 6 after stimulation, cells were stained with anti-CD4 Ab and COS-7-expressed I-A^b-Env tetramer or the I-A^b tetramer containing the A/NT/60/68 $NP_{413-435}$ epitope and were analyzed by flow cytometry. Cells are gated on live $CD4^+$ lymphocytes. *B*, Representative FACS profiles of cells from inguinal draining lymph node (DLN), spleen, and lesion (tumor upon MoMSV infection, lung upon influenza A/NT/60/68 infection), either 14 days postinfection with MoMSV or 8 days postinfection with influenza A/NT/60/68 virus (25 hemagglutinating units (HAU)), stained with anti-CD4 Ab, 1B11 Ab, and *Drosophila*-expressed I-A^b-Env tetramer. Cells are gated on live $CD4^+$ lymphocytes.

not shown). D^b-tetramers can readily be produced with this triple-substituted epitope (GagL*, Abu-Abu-Leu-Abu-Leu-Thr-Val-Phe-Leu), and these D^b-GagL* tetramers were used to stain lymphocyte populations of MoMSV-infected mice at day 14 postinfection (Fig. 3). D^b-GagL* tetramers stain a high percentage of $CD8^+$ T cells in all organs analyzed (average: 4.29, 6.16, and 13.48% in DLNs, spleen, and lesion, respectively). In contrast, only low levels of staining are observed in noninfected mice and in mice infected with influenza A/NT/60/68 virus (average, 0.16 ± 0.14) (Fig. 3).

Phenotype of MoMSV-specific $CD8^+$ and $CD4^+$ T cells

The ability to visualize the immunodominant $CD4^+$ T cell and $CD8^+$ T cell responses within a single infection model allows the direct comparison of $CD4^+$ and $CD8^+$ T cell immunity, with respect to features such as phenotype, distribution, and kinetics. Both Ag-specific $CD4^+$ and $CD8^+$ T cells were found to display a phenotype characteristic for effector and memory T cells, as defined by low to absent expression of CD62L and high expression of CD44 (Table I). No clear differences were found in the expression of T cell activation markers on the Ag-specific $CD4^+$ or $CD8^+$ T cells isolated from different organs of MoMSV-infected mice. Interestingly, both the Ag-specific $CD4^+$ and $CD8^+$ T cells, defined by MHC tetramer staining, were found to react with the Ab 1B11.

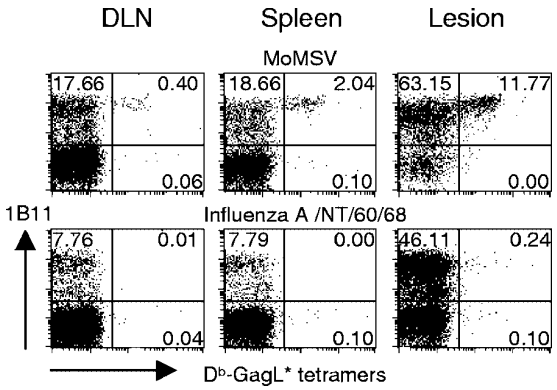

FIGURE 3. Detection of MoMSV-specific $CD8^+$ T cells. Representative FACS profiles of cells from DLN, spleen, and lesion (tumor upon MoMSV infection, lung upon influenza A/NT/60/68 infection) isolated either 14 days postinfection with MoMSV or 8 days postinfection with influenza A/NT/60/68 virus (25 HAU), stained with anti-CD8 Ab, D^b-GagL* tetramer, and 1B11 Ab. Cells are gated on live $CD8^+$ lymphocytes.

The 1B11 Ab has been described to recognize an activation-associated isoform of CD43 (38), which was recently found to be up-regulated on effector $CD8^+$ T cells but absent on memory $CD8^+$ T cells, defining it as a marker for effector phase $CD8^+$ T cells (39). The finding that MoMSV-specific $CD4^+$ T cells, isolated from MoMSV-infected mice, also express 1B11 suggests that this marker may not only be used to detect effector $CD8^+$ T cells, but also to define effector $CD4^+$ T cells. The observation that ~50% (range, 28–93%) of the $CD4^+$ T cells present within the lesion expresses 1B11 at the peak of infection is consistent with this notion (Fig. 2*B*).

Function of MoMSV-specific $CD8^+$ and $CD4^+$ T cells

To determine whether the T cell responses detected by I-A^b-Env and D^b-GagL* tetramer staining correlated with Ag-induced cytokine responses, tissue samples of MoMSV-infected mice were stained separately with tetramers or with anti-IFN-γ Ab upon specific in vitro stimulation (Fig. 4) (combined MHC tetramer staining/intracellular cytokine staining is made impossible by Ag-induced TCR down-regulation). In the majority of organs containing a significant percentage of Ag-specific cells as determined by tetramer staining, Ag-specific IFN-γ staining was likewise detected.

Table I. *Phenotype of MoMSV-specific $CD4^+$ and $CD8^+$ T cells*[a]

Marker	Site	$CD8^+D^b$-GagL*$^+$	$CD4^+$I-A^b-Env$^+$
1B11	DLN	85 ± 10	82 ± 6
	Spleen	95 ± 3	76 ± 16
	Lesion	84 ± 16	95 ± 6
CD62L	DLN	26 ± 11	11 ± 6
	Spleen	5 ± 7	7 ± 1
	Lesion	5 ± 7	7 ± 4
CD44	DLN	90 ± 8	96 ± 3
	Spleen	99 ± 1	94 ± 1
	Lesion	94 ± 5	92 ± 13

[a] Isolated inguinal DLN, spleen, and lesion cells of mice 14 days postinfection with MoMSV were stained with either anti-CD8 Ab and D^b-GagL* tetramers or anti-CD4 Ab and *Drosophila*-expressed I-A^b-Env tetramers, together with FITC-labeled 1B11 Ab, anti-CD62L Ab, or anti-CD44 Ab. Percentages (average ± SD) of marker-positive cells within the I-A^b-Env tetramer$^+CD4^+$ T cell and D^b-GagL* tetramer$^+CD8^+$ T cell population are shown. Data are representative for two independent experiments (n = 5, n = 3). On average, 46, 22, and 12 $CD4^+$I-A^b-Env$^+$ cells and 120, 358, and 626 $CD8^+D^b$-GagL*$^+$ cells were counted for DLN, spleen, and lesion, respectively.

In both the $CD4^+$ and $CD8^+$ T cell compartment, the frequency of $tetramer^+$ cells was generally higher than the frequency of Ag-specific cells as revealed by IFN-γ production (on average two-fold). Interestingly, Ag-specific $CD8^+$ T cells in the DLN appear less capable of producing IFN-γ (Fig. 4*B*), possibly indicating that these cells may not have fully differentiated into IFN-γ-producing cells. Further analysis of the cytokine profile of the MoMSV Env-specific $CD4^+$ T cell response by intracellular cytokine staining revealed a Th1 phenotype, as manifested by the production of TNF-α, IL-2, and GM-CSF, but not IL-10 and IL-4 (data not shown).

Kinetics of the MoMSV-specific $CD8^+$ and $CD4^+$ T cell response

We subsequently compared the kinetics and distribution of the MoMSV-specific $CD4^+$ and $CD8^+$ T cell response during primary MoMSV infection. Early in the response (day 10 postinfection), comparable percentages of MoMSV-specific $CD4^+$ T cells (1.12%) and MoMSV-specific $CD8^+$ T cells (0.71%) are detected at site of infection (Fig. 5*A*). Subsequently, the MoMSV-specific $CD8^+$ T cell response increases dramatically, whereas the MoMSV-specific $CD4^+$ T cell response is either constant or decreases slightly (22.25 and 0.72%, respectively, on day 17). To quantify this shift in T cell immunity, the absolute numbers of MoMSV-specific $CD4^+$ and $CD8^+$ T cells were determined at different time points after infection (Fig. 5*B*). At day 10 after infection, the lesion contains comparable numbers of MoMSV-specific $CD4^+$ T cells (5.9×10^3) and $CD8^+$ T cells (8.4×10^3). Subsequently, the expansion of MoMSV-specific $CD8^+$ T cells outpaces that of MoMSV-specific $CD4^+$ T cells, and at day 14 GagL-specific $CD8^+$ T cells outnumber Env-specific $CD4^+$ T cells by >75-fold.

A comparable shift in both frequency and absolute numbers of MoMSV-specific $CD4^+$ and $CD8^+$ T cells appears to take place in DLN and spleen (Fig. 5). Although the frequencies/absolute numbers of Ag-specific $CD4^+$ and $CD8^+$ T cells at day 10 after infection are too close to background levels in these organs to accurately determine the relative contribution of the different subsets at this early time point, similar numbers of Ag-specific $CD4^+$ and $CD8^+$ T cells appear present at both sites. In contrast, at day 14 postinfection, GagL-specific $CD8^+$ T cells outnumber Env-specific $CD4^+$ T cells by ~23- and 34-fold in DLN and spleen, respectively. Collectively, these data show a shift from combined $CD4^+$ and $CD8^+$ T cell immunity early in the MoMSV-specific T cell response, toward a T cell response that is dominated by $CD8^+$ T cells at the peak of infection (Fig. 5*C*).

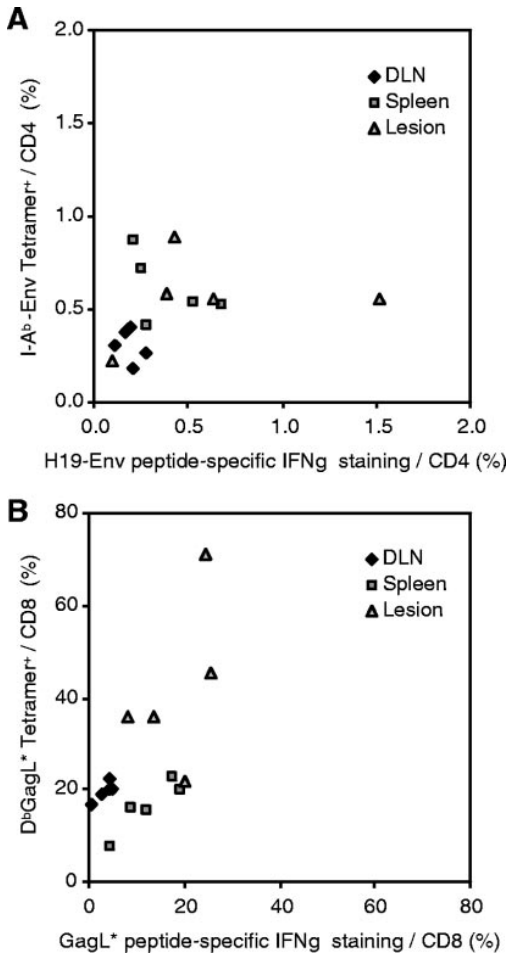

FIGURE 4. Correlation of $tetramer^+$ and IFN-γ^+ T cell responses. Purified DLN (diamonds), spleen (squares), and lesion (triangles) cells of mice ($n = 5$) 17 days postinfection with MoMSV were stained with anti-CD4 Ab and *Drosophila*-expressed $I\text{-}A^b$-Env or anti-CD8 Ab and D^b-GagL* tetramers. In parallel, cell suspensions from the same tissue samples were stimulated for 4 h at 37°C in the presence of 10 U/ml IL-2 and H19-Env peptide, GagL* peptide, or no peptide and were subsequently stained for CD4/CD8 and intracellular IFN-γ expression. H19-Env/GagL*-specific IFN-γ staining was determined by subtracting the background IFN-γ staining (IFN-γ staining after stimulation in the absence of peptide) from the IFN-γ staining after specific stimulation with peptide. Data show the percentage of tetramer-positive cells within the $CD4^+CD8^+$ T cell compartment vs peptide-specific IFN-γ staining within the $CD4^+CD8^+$ T cell compartment.

A dual role for $CD4^+$ T cells in the regression of MoMSV-induced sarcomas

Prior studies have shown that $CD4^+$ T cells provide stimulatory signals in the generation of Ag-specific $CD8^+$ T cell responses (3, 40–44). To test whether the generation of Ag-specific cytotoxic T cell responses after MoMSV infection is also dependent on $CD4^+$ T cells, we examined the MoMSV-specific $CD8^+$ T cell response in mice lacking $CD4^+$ T cells. CD4 depletion leads to a reduction in the number of GagL*-$tetramer^+$ $CD8^+$ T cells in the DLN and spleen at both day 10 and day 14 after MoMSV infection (day 14, 63 and 53%, $p = 0.005$ and 0.08, respectively; Fig. 6). Likewise, reduced numbers of GagL*-$tetramer^+$ $CD8^+$ T cells are detected in DLN and spleen of $MHCII^{-/-}$ mice (day 14, 81 and 72%, $p = 0.04$ and 0.01, respectively; data not shown). In addition, CD4 depletion leads to a reduction in the number of GagL*-$tetramer^+$ $CD8^+$ T cells in lesions of CD4-depleted mice at day 10 after MoMSV infection (84%, $p = 0.01$, data not shown). Collectively, these data indicate that $CD4^+$ cells contribute significantly to the generation of the MoMSV-specific $CD8^+$ T cell response upon viral infection. In contrast to the reduction in GagL*-$tetramer^+$ $CD8^+$ T cells early in the response, the number of Ag-specific $CD8^+$ cells in the muscle of CD4-depleted mice is increased at day 14 after MoMSV infection (3-fold, $p = 0.01$; Fig. 6), possibly as a consequence of increased viral load in lesions of CD4-depleted mice. Immunohistochemical analysis suggests that these $CD8^+$ T cells may not have infiltrated the infected tissue in CD4-depleted mice (see below).

$CD4^+$ T cell immunity is indispensable for the regression of MoMSV-induced lesions. Although $CD8^+$ T cell immunity contributes to viral clearance, it is not essential. It is therefore apparent that there must be an additional role(s) for Ag-specific $CD4^+$ T cell immunity in sarcoma regression, besides controlling the magnitude of the Ag-specific $CD8^+$ T cell response. In particular, the

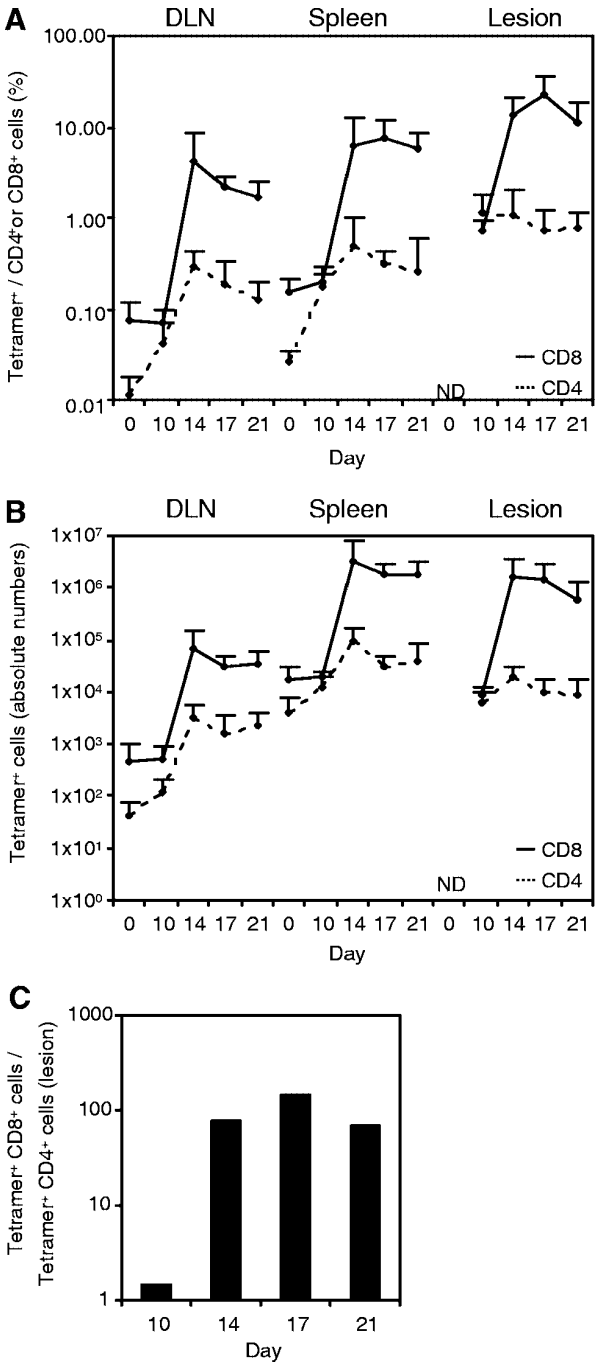

FIGURE 5. Kinetics of MoMSV-specific $CD4^+$ and $CD8^+$ T cell responses. Mice were infected i.m. with MoMSV virus and sacrificed at day 10, 14, 17, or 21 postinfection. Cells from DLN, spleen, and lesion were isolated and stained with either *Drosophila*-expressed I-A^b-Env tetramer/anti-CD4 Ab or D^b-GagL* tetramer/anti-CD8 Ab and were analyzed by flow cytometry. *A*, The percentage (average ± SD) of I-A^b-Env tetramer-positive cells within the $CD4^+$ lymphocyte population and D^b-GagL* tetramer-positive cells within the $CD8^+$ lymphocyte population are depicted. Cells from mediastinal lymph nodes, spleen, and lung of mice on day 8 post-influenza A/NT/60/68 virus infection (25 HAU) showed on average 0.14 ± 0.10% I-A^b-Env $tetramer^+$ and 0.10 ± 0.08% D^b-GagL* $tetramer^+$ cells within the $CD4^+$ and $CD8^+$ T lymphocyte population, respectively. n = 6–7/group; ND = not determined. A significant difference in the kinetics of the percentage of tetramer positive $CD4^+$ and $CD8^+$ T cells was found for all organs analyzed ($p < 0.001$). The median relative increase in the frequency of GagL-specific $CD8^+$ vs Env-specific $CD4^+$ T cells between day 10 and day 14 is 5.1, 8.8, and 18.8; 95% confidence intervals 1.14–22.6, 4.1–18.9, 8.3–42.8 for DLN, spleen, and lesion, respectively. *B*, Absolute numbers of $CD4^+$I-A^b-Env tetramer-positive cells and $CD8^+D^b$-GagL* tetramer-positive cells were calculated from the total number of cells recovered. Averages ± SD are depicted. A significant difference in kinetics of the absolute number of tetramer-positive $CD4^+$ and $CD8^+$ T cells was found for all organs analyzed ($p < 0.002$). The median relative increase in the absolute number of GagL-specific $CD8^+$ T vs Env-specific $CD4^+$ T cells between day 10 and day 14 is 5.1, 11.3, and 31.6; 95% confidence intervals 1.21–21.8, 4.5–28.7, and 12.8–78.1 for DLNs, spleen, and lesion respectively. *C*, Shift in MoMSV-specific T cell immunity during sarcoma regression. Bars represent the ratio of $CD8^+D^b$-GagL* $tetramer^+$ cells/$CD4^+$I-A^b-Env $tetramer^+$ cells in the lesion at the indicated time points, as determined from the absolute numbers of MHC class I and MHC class II tetramer-positive cells.

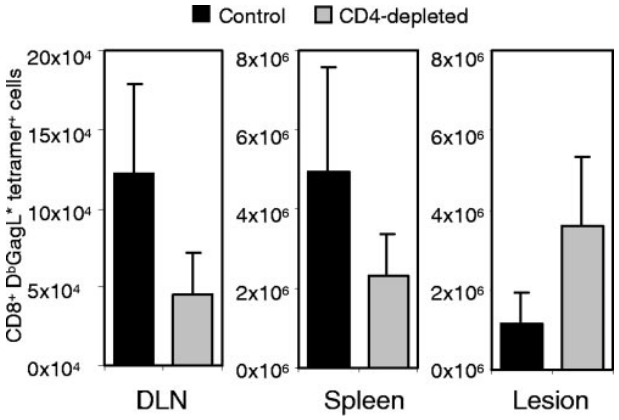

FIGURE 6. CD4-dependent Ag-specific $CD8^+$ T cell response in MoMSV-infected mice. Mice were either left untreated or injected i.p. with 100 μg of anti-CD4 Ab (GK1.5) in 0.2 ml PBS every 2–3 days for the duration of the experiment ($n = 3$ per group). On day 0, mice were infected with MoMSV virus, and at day 14 post infection, cells from DLN, spleen, and lesion were isolated and stained with allophycocyanin-labeled D^b-GagL* tetramer and anti-CD8 Ab and were analyzed by flow cytometry. The absolute numbers (average ± SD) of $CD8^+D^b$-GagL* tetramer-positive cells are shown.

finding that significant numbers of Ag-specific $CD4^+$ T cells accumulate within the lesion early during infection suggests a second possible role for $CD4^+$ T cell immunity at this site. Ag-specific $CD4^+$ T cells within the lesion could mediate direct antiviral effects, as has been described for the related Friend virus (45). Alternatively, these cells might promote tumor regression by "conditioning" of the effector site through the secretion of cytokines or through cell-cell interactions.

Previous studies have provided evidence for an IFN-γ-mediated effect of $CD4^+$ T cells on macrophage function (5), and large numbers of cytotoxic macrophages are present in regressing FMR-induced tumors (16–18, 46–48). To study a possible role of $CD4^+$ T cells on the infiltrate of MoMSV-induced lesions, we performed immunohistochemistry (IHC) on lesions of normal and CD4-depleted MoMSV-infected mice. Sections of infected muscle tissue before onset of regression were stained with anti-CD8 and F4/80 Abs to reveal cytotoxic T cells and macrophages. In addition, sections were stained with anti-I-A^b Ab, as activation and maturation of macrophages are known to be associated with the up-regulation of MHC class II expression. MoMSV-infected muscle tissue is characterized by significant numbers of CD8-positive cells (Fig. 7*A*). In addition, very high numbers of F4/80-positive cells are found, in line with previous reports showing that macrophages are

abundantly present within MoMSV-induced sarcomas (Fig. 7*C*) (16–18).

CD4 depletion results in a decreased infiltration of cells positive for the macrophage marker F4/80 in the lesion (Fig. 7, *C* and *D*). Infiltration of cells that express the dendritic cell marker CD11c or the granulocyte marker Gr1 does not appear decreased significantly (data not shown). In IHC sections of CD4-depleted mice there is a significant reduction of $CD8^+$ cells (Fig. 7, *A* and *B*), even at a time point at which $CD8^+$ numbers as measured by flow cytometry are increased. This difference between $CD8^+$ cell infiltration as measured by flow cytometry and IHC is consistently observed in multiple experiments and may suggest an altered distribution of the $CD8^+$ T cells in lesions of CD4-depleted mice. Further analysis will be required to resolve this issue. Most strikingly, a dramatic reduction in the number of cells expressing MHC class II is observed in sarcomas of CD4-depleted mice (Fig. 7, *E* and *F*). To study which cells express MHC class II in the lesions and how this is affected by CD4 depletion, sections of MoMSV-induced sarcomas were simultaneously stained with F4/80 and anti-$I\text{-}A^b$ Ab (Fig. 7, *G* and *H*). In MoMSV-induced lesions of control mice, colocalization of MHC class II and F4/80 dominates, indicating that most of the MHC class II-expressing cells within the lesion are macrophages and that most of the macrophages within the lesion are activated. In CD4-depleted mice, the picture is strikingly different. Although single positive cells (i.e., $F4/80^+$MHC II^- and $F4/80^-$MHC II^+) are still present, there is a very strong reduction in the number of activated, MHC II^+ macrophages. Because only few $B220^+$ cells and significant numbers of $CD11c^+$ cells are found in the lesion (data not shown), the remaining ($F4/80^-$) MHC II^+ cells are most likely dendritic cells, the accumulation of which appears less dependent on $CD4^+$ T cells. Collectively, these data indicate that $CD4^+$ T cell immunity contributes to the infiltration/accumulation of immune cells and in particular the accumulation and activation of macrophages at the effector site during MoMSV infection.

Discussion

Here we use MHC class II tetramers to characterize the distribution and kinetics of the $CD4^+$ T cell response against the oncoretrovirus MoMSV and compare this response with the $CD8^+$ T cell response. Low but detectable numbers of $I\text{-}A^b$-Env tetramer-positive $CD4^+$ T cells are present in the DLNs of MoMSV-infected mice. In addition, sizeable numbers of Ag-specific $CD4^+$ T cells are detected within lesions of MoMSV-infected mice (Fig. 5*A*). In organs containing a significant percentage of $I\text{-}A^b$-Env $tetramer^+CD4^+$ cells, MoMSV Env-specific IFN-γ staining was likewise detected. The enrichment of (cytokine-producing) Ag-specific $CD4^+$ T cells at the site of infection provides indirect (numerical) support for the notion that provision of T cell help in the draining lymphoid organ is only a single aspect of Ag-specific $CD4^+$ T cell immunity (see below).

The majority of MoMSV-specific $CD4^+$ T cells detected by MHC tetramer staining are of an effector/memory phenotype as defined by the expression levels of CD62L and CD44. Interestingly, a large fraction of Ag-specific $CD4^+$ T cells express the 1B11-reactive, activation-induced isoform of CD43 that was recently shown to define effector $CD8^+$ T cell populations. Based on these data it is plausible that the 1B11 marker can also be used to define effector $CD4^+$ T cells, but formal proof for this will require functional analysis of $1B11^+$ and $1B11^-$ Ag-specific $CD4^+$ T cells at different time points after infection. Although virtually all MHC class I and MHC class II tetramer-positive cells were $1B11^+$, MHC $tetramer^+$ cells constituted only 1–2% and 9–16% of the $1B11^+CD4^+$ and $1B11^+CD8^+$ T cells, respectively. This is unlikely to be a result of the presence of large numbers of Ag-specific T cells that are directed against other MoMSV-derived epitopes, as the epitopes used in this study have been previously characterized as the immunodominant epitopes in the T cell response against FMR retroviruses (Ref. 37 and F. Ossendorp, unpublished data). The finding that MHC $tetramer^+$ cells constitute only a minor fraction of activated ($1B11^+$) cells might conceivably be due to the lack of MHC tetramers to identify all Ag-specific cells. In a number of viral infection systems, a failure of MHC class I tetramers to identify all Ag-specific $CD8^+$ T cells has been demonstrated, in particular in situations of high viral load (49, 50). Likewise, it has previously been described for $CD4^+$ T cell clones in a number of different systems that MHC class II tetramers containing the antigenic peptide fail to stain a subset of (low-avidity) Ag-specific hybridomas (10, 12). In line with this, we found that $I\text{-}A^b$-Env tetramers do not bind to a previously characterized Env-specific $CD4^+$ T cell clone (Ref. 24 and data not shown). However, the finding that MHC tetramers and intracellular cytokine staining identify similar numbers of Ag-specific $CD4^+$ and $CD8^+$ T cells argues against an underestimate of T cell responses as measured by MHC tetramer staining. The $1B11^+$ MHC tetramer-negative T cell populations might consist of Ag-specific T cells that have become refractory to both MHC tetramer staining and Ag-specific cytokine production. Alternatively, they may consist of bystander T (memory) cells activated by the inflammatory conditions, two possible explanations that deserve further study.

Previously, Ag-specific $CD4^+$ T cell frequencies have been estimated by indirect enumeration, using limiting dilution assays,

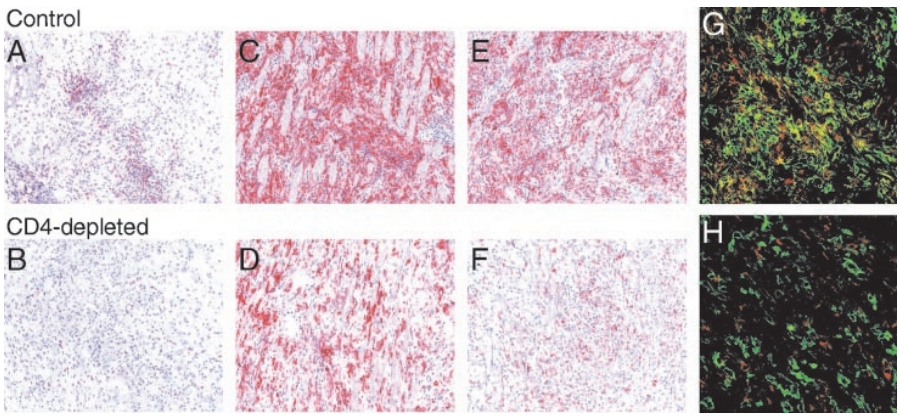

FIGURE 7. Immunohistochemistry of MoMSV-induced lesions of normal B6 and CD4-depleted mice. At day 14 postinfection, lesions of untreated and CD4-depleted C57BL/6 mice were isolated, sectioned, and stained with anti-CD8 (*A* and *B*), F4/80 (*C* and *D*), anti-$I\text{-}A^b$ (*E* and *F*), or anti-$I\text{-}A^b$ and F4/80 Abs (*G* and *H*). *G* and *H*, Colored overlay of F4/80 expression (green) and I-Ab expression (red). Coexpression leads to an orange-yellow coloring. Original magnifications, ×200 (*A–F*) and ×400 (*G* and *H*). Pictures are representative for seven individual mice in each group.

ELISPOT and intracellular cytokine staining. These studies suggested that, as based on functional assays, the frequencies of Ag-specific $CD4^+$ T cells are considerably lower than the frequencies of Ag-specific $CD8^+$ T cells (8, 51, 52). Both the results by Homann et al. (15), which use tetramer technology to analyze the LCMV-specific $CD4^+$ and $CD8^+$ T cell reponse, and the results described here support the idea that the number of virus-specific $CD4^+$ T cells are indeed considerably lower ($\sim$20–40) than the number of virus-specific $CD8^+$ T cells.

The most striking observation from the comparison of the epitope-specific $CD4^+$ and $CD8^+$ T cell responses is the pronounced shift toward a $CD8^+$ T cell-dominated T cell response at the site of infection. Early during MoMSV infection, the MoMSV-specific T cell response at the effector site is of comparable size in the $CD4^+$ and $CD8^+$ T cell compartment, whereas at later stages of infection, GagL*-specific $CD8^+$ T cells outnumber Env-specific $CD4^+$ T cells by 75-fold. Because these two epitopes appear immunodominant in the T cell response against FMR retroviruses (Ref. 37 and F. Ossendorp, unpublished data), this likely reflects the kinetics of the entire MoMSV-specific T cell response. In line with this, a similar, albeit less dramatic, shift in the total CD4 $1B11^+$:CD8 $1B11^+$ ratio is observed within the lesion during the course of regression ($CD4^+1B11^+$:$CD8^+1B11^+$ ratio day 10 1:3.5; $CD4^+1B11^+$:$CD8^+1B11^+$ ratio day 14 1:9.4).

The shift toward a $CD8^+$ T cell-dominated T cell response during the progression of MoMSV infection is unlikely to be a consequence of differences in migration properties of MoMSV-specific $CD4^+$ and $CD8^+$ T cells as GagL-specific $CD8^+$ T cells outnumber Env-specific $CD4^+$ T cells in all three organs analyzed during the peak of the response. However, other intrinsic differences between $CD4^+$ and $CD8^+$ T cell responses may contribute to the observed kinetic difference. Recently, Foulds et al. (53) demonstrated that $CD4^+$ T cells are programmed to divide a limited number of times upon Ag exposure. In addition, Ag-specific $CD4^+$ T cells may be more susceptible to apoptosis, as previously has been suggested for memory $CD4^+$ T cells (15). Furthermore, encounter of high Ag concentrations can result in T cell anergy and concurrent loss of MHC class II tetramer binding in in vitro assays (54).

In addition to a possible contribution of such lineage-intrinsic differences, pathogen-specific factors are likely to affect the kinetics of Ag-specific $CD4^+$ and $CD8^+$ T cell immunity. Indeed, the observation that a kinetic difference between primary $CD4^+$ and $CD8^+$ T cell responses is not apparent during LCMV infection (15) could indicate that pathogen-specific factors may exert an overriding effect. Such pathogen-specific factors could include the kinetics of epitope generation but also the precursor frequency of the pathogen-reactive $CD4^+$ and $CD8^+$ T cell compartment. The ability to mount an early $CD4^+$ T cell response may be essential for the development of protective immunity against certain pathogens. Prior studies have revealed that $I\text{-}A^b$ is a protective MHC class II allele during FMR infection, and the current data suggest that this may be a reflection of the rapid $CD4^+$ T cell response against FMR Env-$I\text{-}A^b$ complexes. Likewise, the ability to mount an early CMV-specific $CD4^+$ T cell response appears to correlate with a favorable clinical course during primary CMV infection in transplant recipients (L. Gamadia, personal communication).

As has been previously shown in other models (3, 40–44), $CD4^+$ T cells promote the generation of Ag-specific $CD8^+$ T cell immunity during MoMSV infection. This role of $CD4^+$ T cells might be mediated either via a direct effect of $CD4^+$ T cell-secreted cytokines/chemokines or through the licensing of APCs. A second role for $CD4^+$ T cell immunity is suggested by the accumulation of significant numbers of Ag-specific $CD4^+$ T cells within the lesion early during infection. These $CD4^+$ cells contribute to the inflammatory environment in the lesion by promoting the accumulation of large numbers of macrophages and by mediating the activation of these macrophages as revealed by MHC class II expression, possibly through IFN-γ secretion (5, 55–57). Collectively, these data provide support for a central role of $CD4^+$ T cell immunity both in the initiation of $CD8^+$ T cell immunity and in the interplay between acquired and innate immunity. It will be challenging to dissect the various facets of $CD4^+$ T cell immunity in human disease conditions associated with diminished $CD4^+$ T cell counts, such as Epstein Barr virus$^+$ B cell lymphomas and cytomegalovirus disease.

Acknowledgments

We thank Helmut Kessels for peptide synthesis, Marcel Camps and Laura Ribeiro for help with the analysis of the CD4-depleted mice, the members of the Schumacher lab for discussions, A. Kruisbeek and H. Spits for critically reading the manuscript, and Guus Hart for statistical analysis.

References

1. Bennett, S. R., F. R. Carbone, F. Karamalis, R. A. Flavell, J. F. Miller, and W. R. Heath. 1998. Help for cytotoxic-T-cell responses is mediated by CD40 signalling. *Nature 393:478.*
2. Ridge, J. P., R. F. Di, and P. Matzinger. 1998. A conditioned dendritic cell can be a temporal bridge between a $CD4^+$ T-helper and a T-killer cell. *Nature 393: 474.*
3. Schoenberger, S. P., R. E. Toes, E.I. van der Voort, R. Offringa, and C. J. Melief. 1998. T-cell help for cytotoxic T lymphocytes is mediated by CD40-CD40L interactions. *Nature 393:480.*
4. Hasenkrug, K. J., and U. Dittmer. 2000. The role of CD4 and CD8 T cells in recovery and protection from retroviral infection: lessons from the Friend virus model. *Virology 272:244.*
5. Hung, K., R. Hayashi, W. A. Lafond, C. Lowenstein, D. Pardoll, and H. Levitsky. 1998. The central role of $CD4^+$ T cells in the antitumor immune response. *J. Exp. Med. 188:2357.*
6. Qin, Z., and T. Blankenstein. 2000. $CD4^+$ T cell-mediated tumor rejection involves inhibition of angiogenesis that is dependent on IFNγ receptor expression by nonhematopoietic cells. *Immunity 12:677.*
7. Cerundolo, V. 2000. Use of major histocompatibility complex class I tetramers to monitor tumor-specific cytotoxic T lymphocyte response in melanoma patients. *Cancer Chemother. Pharmacol. 46:S83.*
8. Doherty, P. C., and J. P. Christensen. 2000. Accessing complexity: the dynamics of virus-specific T cell responses. *Annu. Rev. Immunol. 18:561.*
9. Kotzin, B. L., M. T. Falta, F. Crawford, E. F. Rosloniec, J. Bill, P. Marrack, and J. Kappler. 1999. Use of soluble peptide-DR4 tetramers to detect synovial T cells specific for cartilage antigens in patients with rheumatoid arthritis. *Proc. Natl. Acad. Sci. USA 97:291.*
10. Rees, W., J. Bender, T. K. Teague, R. M. Kedl, F. Crawford, P. Marrack, and J. Kappler. 1999. An inverse relationship between T cell receptor affinity and antigen dose during $CD4^+$ T cell responses in vivo and in vitro. *Proc. Natl. Acad. Sci. USA 96:9781.*
11. Savage, P. A., J. J. Boniface, and M. M. Davis. 1999. A kinetic basis for T cell receptor repertoire selection during an immune response. *Immunity 10:485.*
12. Meyer, A. L., C. Trollmo, F. Crawford, P. Marrack, A. C. Steere, B. T. Huber, J. Kappler, and D. A. Hafler. 2000. Direct enumeration of *Borrelia*-reactive CD4 T cells ex vivo by using MHC class II tetramers. *Proc. Natl. Acad. Sci. USA 97:11433.*
13. Novak, E. J., A. W. Liu, G. T. Nepom, and W. W. Kwok. 1999. MHC class II tetramers identify peptide-specific human $CD4^+$ T cells proliferating in response to influenza A antigen. *J. Clin. Invest. 104:R63.*
14. Kwok, W. W., A. W. Liu, E. J. Novak, J. A. Gebe, R. A. Ettinger, G. T. Nepom, S. N. Reymond, and D. M. Koelle. 2000. HLA-DQ tetramers identify epitope-specific T cells in peripheral blood of herpes simplex virus type 2-infected individuals: direct detection of immunodominant antigen-responsive cells. *J. Immunol. 164:4244.*
15. Homann, D., L. Teyton, and M. B. Oldstone. 2001. Differential regulation of antiviral T-cell immunity results in stable $CD8^+$ but declining $CD4^+$ T-cell memory. *Nat. Med. 7:913.*
16. Fefer, A., J. L. McCoy, K. Perk, and J. P. Glynn. 1968. Immunologic, virologic, and pathologic studies of regression of autochthonous Moloney sarcoma virus-induced tumors in mice. *Cancer Res. 28:1577.*
17. Stanton, M. F., L. W. Law, and R. C. Ting. 1968. Some biologic, immunogenic, and morphologic effects in mice after infection with a murine sarcoma virus. II. Morphologic studies. *J. Natl. Cancer Inst. 40:1113.*
18. Becker, S., and S. Haskill. 1981. Kinetics of inflammation and sarcoma cell development in primary Moloney sarcoma-virus-induced tumors. *Int. J. Cancer 27:229.*
19. Collavo, D., A. Colombatti, and B. L. Chieco. 1974. T lymphocyte requirement for MSV tumour prevention or regression. *Nature 249:169.*
20. De Clercq, E. 1975. Tumor induction by Moloney sarcoma virus in athymic nude mice. *J. Natl. Cancer Inst. 54:473.*
21. Stutman, O. 1975. Immunodepression and malignancy. *Adv. Cancer Res. 22:261.*

22. Bateman, W. J., E. J. Jenkinson, and J. J. Owen. 1987. T-cell immunity to murine Moloney sarcoma virus-induced tumours: L3T4$^+$ T cells are necessary for resistance to primary sarcoma growth, but Lyt-2$^+$ T cells are required for resistance to secondary tumour cell challenge. *Immunology 61:317.*
23. Biasi, G., M. Mazzocchi, A. Facchinetti, M. Panozzo, P. Zanovello, D. Collavo, and B. L. Chieco. 1990. Induction of Moloney murine sarcoma virus tolerance in adult mice by anti-CD4 monoclonal antibody treatment. *Cancer Res. 50:57035.*
24. Ossendorp, F., E. Mengede, M. Camps, R. Filius, and C. J. Melief. 1998. Specific T helper cell requirement for optimal induction of cytotoxic T lymphocytes against major histocompatibility complex class II negative tumors. *J. Exp. Med. 187:693.*
25. Stukart, M. J., A. Vos, and C. J. Melitef. 1981. Cytotoxic T cell response against lymphoblasts infected with Moloney (Abelson) murine leukemia virus: methodological aspects and H-2 requirements. *Eur. J. Immunol. 11:251.*
26. Altman, J. D., P. A. Moss, P. J. Goulder, D. H. Barouch, W. M. McHeyzer, J. I. Bell, A. J. McMichael, and M. M. Davis. 1996. Phenotypic analysis of antigen-specific T lymphocytes. *Science 274:94.*
27. Haanen, J. B., M. Toebes, T. A. Cordaro, M. C. Wolkers, A. M. Kruisbeek, and T. N. Schumacher. 1999. Systemic T cell expansion during localized viral infection. *Eur. J. Immunol. 29:1168.*
28. Lyons, A. B., and C. R. Parish. 1994. Determination of lymphocyte division by flow cytometry. *J. Immunol. Methods 171:131.*
29. Murali, K. K., J. D. Altman, M. Suresh, D. J. Sourdive, A. J. Zajac, J. D. Miller, J. Slansky, and R. Ahmed. 1998. Counting antigen-specific CD8 T cells: a reevaluation of bystander activation during viral infection. *Immunity 8:177.*
30. Vyth, D. F., H. Boot, T. A. Dellemijn, D. M. Majoor, L. C. Oomen, J. D. Laman, M. M. Van, W. R. De, and J. D. De. 1998. Localization in situ of costimulatory molecules and cytokines in B-cell non-Hodgkin's lymphoma. *Immunology 94: 580.*
31. Vyth, D. F., T. A. Dellemijn, D. Majoor, and J. D. De. 1995. Localization in situ of the co-stimulatory molecules B7.1, B7.2, CD40 and their ligands in normal human lymphoid tissue. *Eur. J. Immunol. 25:3023.*
32. van den Broek, M. F., D. Kagi, F. Ossendorp, R. Toes, S. Vamvakas, W. K. Lutz, C. J. Melief, R. M. Zinkernagel, and H. Hengartner. 1996. Decreased tumor surveillance in perforin-deficient mice. *J. Exp. Med. 184:1781.*
33. Cerundolo, V., T. Lahaye, C. Horvath, P. Zanovello, D. Collavo, and H. D. Engers. 1987. Functional activity in vivo of effector T cell populations. III. Protection against Moloney murine sarcoma virus (M-MSV)-induced tumors in T cell deficient mice by the adoptive transfer of a M-MSV-specific cytolytic T lymphocyte clone. *Eur. J. Immunol. 17:173.*
34. Iwashiro, M., T. Kondo, T. Shimizu, H. Yamagishi, K. Takahashi, Y. Matsubayashi, T. Masuda, A. Otaka, N. Fujii, A. Ishimoto, et al. 1993. Multiplicity of virus-encoded helper T-cell epitopes expressed on FBL-3 tumor cells. *J. Virol. 67:4533.*
35. O'Shea, E. K., K. J. Lumb, and P. S. Kim. 1993. Peptide "Velcro" design of a heterodimeric coiled coil. *Curr. Biol. 3:658.*
36. Gao, X. M., F. Y. Liew, and J. P. Tite. 1989. Identification and characterization of T helper epitopes in the nucleoprotein of influenza A virus. *J. Immunol. 143: 3007.*
37. Chen, W., H. Qin, B. Chesebro, and M. A. Cheever. 1996. Identification of a gag-encoded cytotoxic T-lymphocyte epitope from FBL-3 leukemia shared by Friend, Moloney, and Rauscher murine leukemia virus-induced tumors. *J. Virol. 70:7773.*
38. Jones, A. T., B. Federsppiel, L. G. Ellies, M. J. Williams, R. Burgener, V. Duronio, C. A. Smith, F. Takei, and H. J. Ziltener. 1994. Characterization of the activation-associated isoform of CD43 on murine T lymphocytes. *J. Immunol. 153:3426.*
39. Harrington, L. E., M. Galvan, L. G. Baum, J. D. Altman, and R. Ahmed. 2000. Differentiating between memory and effector CD8 T cells by altered expression of cell surface O-glycans. *J. Exp. Med. 191:1241.*
40. Keene, J. A., and J. Forman. 1982. Helper activity is required for the in vivo generation of cytotoxic T lymphocytes. *J. Exp. Med. 155:768.*
41. Husmann, L. A., and M. J. Bevan. 1988. Cooperation between helper T cells and cytotoxic T lymphocyte precursors. *Ann NY Acad. Sci. 532:158.*
42. Cardin, R. D., J. W. Brooks, S. R. Sarawar, and P. C. Doherty. 1996. Progressive loss of CD8$^+$ T cell-mediated control of a γ-herpesvirus in the absence of CD4$^+$ T cells. *J. Exp. Med. 184:863.*
43. von Herrath, M., M. Yokoyama, J. Dockter, M. B. Oldstone, and J. L. Whitton. 1996. CD4-deficient mice have reduced levels of memory cytotoxic T lymphocytes after immunization and show diminished resistance to subsequent virus challenge. *J. Virol. 70:1072.*
44. Bennett, S. R., F. R. Carbone, F. Karamalis, J. F. Miller, and W. R. Heath. 1997. Induction of a CD8$^+$ cytotoxic T lymphocyte response by cross-priming requires cognate CD4$^+$ T cell help. *J. Exp. Med. 186:65.*
45. Iwashiro, M., K. Peterson, R. J. Messer, I. M. Stromnes, and K. J. Hasenkrug. 2001. CD4$^+$ T cells and γ interferon in the long-term control of persistent friend retrovirus infection. *J. Virol. 75:52.*
46. Russell, S. W., and A. T. McIntosh. 1977. Macrophages isolated from regressing: Moloney sarcomas are more cytotoxic than those recovered from progressing sarcomas. *Nature 268:69.*
47. Becker, S., and S. Haskill. 1980. Non-T-cell-mediated cytotoxicity in MSV tumor-bearing mice. III. Macrophage-mediated cytotoxicity against autochthonous MSV tumor-isolated target cells. *Int. J. Cancer 25:535.*
48. Greenberg, P. D. 1991. Adoptive T cell therapy of tumors: mechanisms operative in the recognition and elimination of tumor cells. *Adv. Immunol. 49:281.*
49. Welsh, R. M. 2001. Assessing CD8 T cell number and dysfunction in the presence of antigen. *J. Exp. Med. 193:F19.*
50. Reignat, S., G. J. Webster, D. Brown, G. S. Ogg, A. King, S. L. Seneviratne, G. Dusheiko, R. Williams, M. K. Maini, and A. Bertoletti. 2002. Escaping high viral load exhaustion: CD8 cells with altered tetramer binding in chronic hepatitis B virus infection. *J. Exp. Med. 195:1089.*
51. Maini, M. K., G. Casorati, P. Dellabona, A. Wack, and P. C. Beverley. 1999. T-cell clonality in immune responses. *Immunol. Today 20:262.*
52. Whitmire, J. K., and R. Ahmed. 2000. Costimulation in antiviral immunity: differential requirements for CD4$^+$ and CD8$^+$ T cell responses. *Curr. Opin. Immunol. 12:448.*
53. Foulds, K. E., L. A. Zenewicz, D. J. Shedlock, J. Jiang, A. E. Troy, and H. Shen. Cutting edge: CD4 and CD8 T cells are intrinsically different in their proliferative responses. *J. Immunol. 168:1528.*
54. Cameron, T. O., J. R. Cochran, D. B. Yassine, R. P. Sekaly, and L. J. Stern. 2001. Cutting edge: detection of antigen-specific CD4$^+$ T cells by HLA-DR1 oligomers is dependent on the T cell activation state. *J. Immunol. 166:741.*
55. Buchmeier, N. A., and R. D. Schreiber. 1985. Requirement of endogenous interferon-γ production for resolution of *Listeria* monocytogenes infection. *Proc. Natl. Acad. Sci. USA 82:7404.*
56. Dalton, D. K., M. S. Pitts, S. Keshav, I. S. Figari, A. Bradley, and T. A. Stewart. 1993. Multiple defects of immune cell function in mice with disrupted interferon-γ genes. *Science 259:1739.*
57. Huang, S., W. Hendriks, A. Althage, S. Hemmi, H. Bluethmann, R. Kamijo, J. Vilcek, R. M. Zinkernagel, and M. Aguet. 1993. Immune response in mice that lack the interferon-γ receptor. *Science 259:1742.*